JOURNAL OF MATERIALS SCIENCE **37** (2002) 4633–4643

Oxidation barriers on SiC particles for use in aluminium matrix composites manufactured by casting route: Mechanisms of interfacial protection

A. UREÑA, M. D. ESCALERA, L. GIL
Departamento de Ciencias Experimentales e Ingeniería, Escuela Superior de Ciencias Experimentales y Tecnología, Universidad Rey Juan Carlos, 28933 Móstoles Madrid, Spain

This paper is centred on a study of the interface reaction mechanisms which participate in the fabrication of an aluminium-SiC composite by a casting route, when reinforcements (particles, in this case) have been previously coated by oxidation with a SiO_2 layer. The studies, which were carried out using transmission electron microscopy and differential scanning calorimetry, made it possible to propose a model of action of the SiO_2 barrier in relation to the coating thickness and the reaction time. The first reaction that occurred in this SiC-SiO_2-molten Al system was the formation of an Al-Si-O glassy phase which progressively consumed the SiO_2 barrier, reducing the matrix-particle interface energy and favouring wetting of the SiC surfaces. When the oxidation coating was completely consumed, the SiC was preferentially dissolved by the glassy phase, inside which the formation of amorphous carbon was detected. These studies also show that carbon enrichment of the reaction layer activated the precipitation of metallic impurities (such as Fe or Cu) in the reaction. Longer reaction times (8 h) could also favour crystallization of the glassy phase to form mullite and the formation of microcrystalline alumina at the reaction interface.

1. Introduction

The application of coatings on ceramic reinforcements is a potential solution to control of the interfacial reactivity in discontinuous reinforced aluminium matrix composites (DR-AMC). Of the possible types of protection barrier tested in the design of metal matrix composites, active diffusion coatings present important advantages over more conventional inert diffusion barriers. An active diffusion barrier must be able to react, in a controlled way, with one of the components of the composite, generally the metallic matrix. With this kind of behaviour, two main objectives can be accomplished: (1) to prevent matrix elements reaching and reacting with the ceramic reinforcements [1] and (2) to reduce the matrix-reinforcement interfacial energy by formation of a stable phase, favouring wettability between both composite constituents in a casting procedure [2].

Fig. 1 schematizes the role played by an active diffusion barrier located between the matrix and the reinforcement, as compared with the evolution in the same system when no protection barrier or an inert diffusion barrier is used [1]. The main difference between the two kinds of diffusion barrier is that the inert one has an unlimited service life and is able to reduce the growth rate of the reaction zone, but it does not protect the reinforcement against chemical etching. In contrast with this, an active diffusion barrier has a limited service life and causes rapid growth of the interface reaction products, but it is able to provide complete protection (for a given incubation time) of the reinforcement against chemical etching.

During this incubation period, the active barrier reacts with the metallic matrix but not with the reinforcement. The ceramic phase will only react when all the protective coating has been consumed. When that happens, the active barrier has been converted into reaction products which are usually inert with respect to the matrix and the reinforcement, although in some cases they could react in a controlled way. The main advantage of the active diffusion barrier is that there is a true incubation period during which the reinforcement is completely protected against any chemical interaction.

The application of a protection barrier on ceramic reinforcement used for manufacturing metal matrix composites is quite a common practice. However, most of the outstanding results have been achieved working with continuous reinforcements (SiC fibres) and in highly reactive matrices (Ti alloys or intermetallic phases, such as $TiAl_3$). The latest studies carried out on the Ti/SiCf system include the development of a duplex barrier of C/TiB_x [3] or Ti/C [4], duplex metallic coating of Cu/Mo, Cu/W o Ag-Ta [5, 6], or ceramic coating of yttrium and magnesium oxide [7, 8]. In all cases, CVD, PVD, etc. are used to generate the barrier.

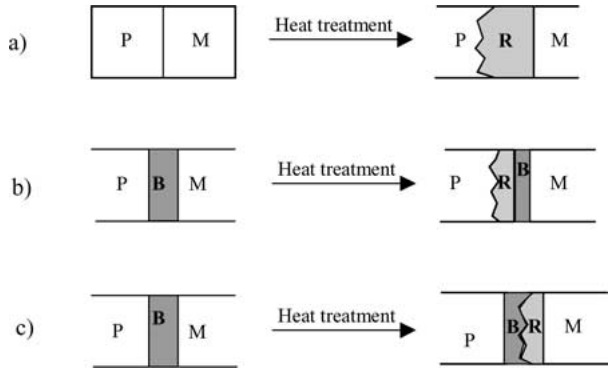

Figure 1 Schematic representation of the matrix-reinforcement interaction: (a) without reinforcement protection, (b) with an inert diffusion barrier, (c) with an active diffusion barrier. P: particle; M: matrix; B: diffusion barrier; R: reaction zone.

However, the solutions developed in those cases are too complex and entail high production costs, so that they would not be acceptable for composites with discontinuous reinforcements. One typical example of a medium reactive system is Al/SiC. The chemical interaction of discontinuous reinforcement of SiC (particles or whiskers) during liquid processing of composites has been studied in depth by several researchers, including the present authors [9–11]. Different solutions have been proposed both for protection against interfacial degradation and for increasing the wettability between molten aluminium and SiC: surface treatments with K_2ZrF_6 aqueous solution of SiC particles to improve their wetting by molten light alloys at low temperatures (700 a 900°C) [12]; the production of an inert ceramic coating (Al_2O_3, ZrO_2, TiO_2) on SiC particles and whiskers by sol-gel method to reduce interface degradation by aluminium carbide formation [13–15]; and coating of discontinuous reinforcements with a metallic barrier such as Ni [16–19], NiP [16, 20] or Cu [21, 22] intended to control reactivity and increase wettability through the formation of an intermediate reaction layer, although in most cases there is some loss of ductility in the composite.

To control the interfacial damage produced during melting of these composites, the authors have proposed a direct oxidation procedure to develop a continuous SiO_2 layer on the SiC particles, which acts as a protection barrier, preventing particle-matrix interface reaction and enhancing the wetting behaviour of the ceramic phase [23].

The object of this paper was to study the mechanisms by which this protection barrier works and to show its nature as an active diffusion barrier. Several reaction models are proposed, based on interfacial observation using transmission electron microscopic techniques such as: conventional TEM, high resolution electron microscopy (HREM), and field emission transmission electron microscopy (FEG-TEM). Other analytical techniques such as differential thermal analysis (DTA) were used to determine such interface mechanisms.

2. Experimental procedure

Microscopic and microanalytical studies to analyse the interfacial chemistry between molten aluminium and oxidized SiC particles, Al/SiC$(SiO_2)_p$ were carried out on specimens constituted by compacted mixtures of aluminium powder (99.7% Al) and 30% volume of pre-oxidized SiC particles (1200°C for 2 and 8 h) with an average size of 26.2 μm. Specimens were subjected to interfacial reaction tests consisting of melting under high vacuum ($<10^{-4}$ Pa) at 900°C, with holding times of 20 and 60 min. Detailed characteristics of the parent material and of the structure and growth kinetic of the oxidized barrier are given in the first part of this paper [23].

After interfacial reaction tests, specimens were prepared for TEM. Specimen preparation consisted of the following operations: (1) cutting of the melted composites into 0.5 mm thick slices using a diamond disc; (2) mechanical grinding of the slices on SiC paper (1200 grade) in ethylene-glycol down to 100 μm; (3) ultrasonic cutting of a 3 mm-diameter disc; (4) mechanical thinning of the disk in ethylene-glycol with 2000 and 4000 grade SiC emery paper down to 50 μm; (5) dimpling at the centre of the disc, using 3 and 1 μm diamond pastes, to reduce minimum sample thickness to a range of 15–20 μm; and (6) ion milling using an Ar^+ ion beam with gun voltage 5 kV, incident angle 15° and thinning times 20–40 h. The specimen stage was cooled with liquid nitrogen.

Prepared specimens were observed with the following transmission electron microscopes: a *Jeol 2000 EX* (200 kV) equipped with an EDS analyser, up to 3.1 Å structural resolution; a *Jeol JEM 4000 EX* high resolution electron microscope with 1.8 Å structural resolution; and a *Philips CM200 FEG 200 KV* field emission transmission electron microscope allowing 2.2 Å resolution between planes. This system was also equipped with an EDS microanalyser.

To complete this study, differential thermal analysis (DTA) were carried out on compacted mixtures of Al with 30% vol SiC powders (approximately 50 mg). In this case, for comparative proposes, specimens were tested with pre-oxidized and with as-received SiC particles. The DSC conditions were: heating from room temperature to 1500°C (rate 10°C/min) under a protective Argon atmosphere (gas flow of 2 l/min).

3. Results

The interphase generated by the interposition of the protection barrier Al/SiO_2/SiC is constituted first by a double interface and then by two different reaction sites: the interfaces Al/SiO_2 and SiO_2/SiC. Previous studies carried out by Hughes *et al*. [24] have shown than at the tested temperature (900°C), the silica and the silicon carbide do not react themselves. In fact, the phase diagram SiO_2-SiC calculated by Weiss *et al*. [25] shows that there is no interaction between the SiC and the silica up to temperatures over 1723°C. For that reason, the main interest in this reactive system is reduced to analysing the reaction that occurs at the Al/SiO_2 interface, and afterwards the secondary reaction that takes place between the SiC and the reactive products formed at the Al/SiO_2 interface, when the protective barrier is completely consumed.

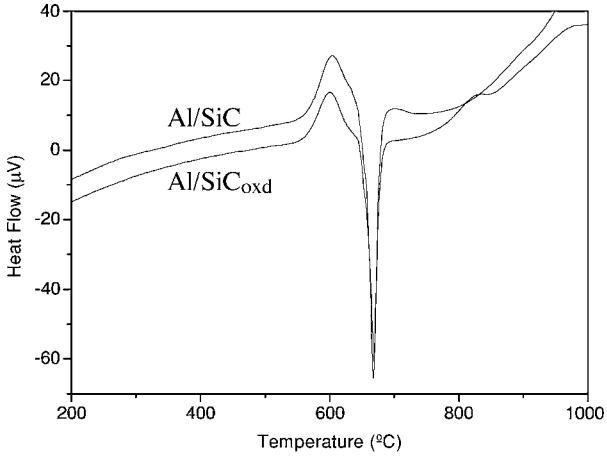

(a)

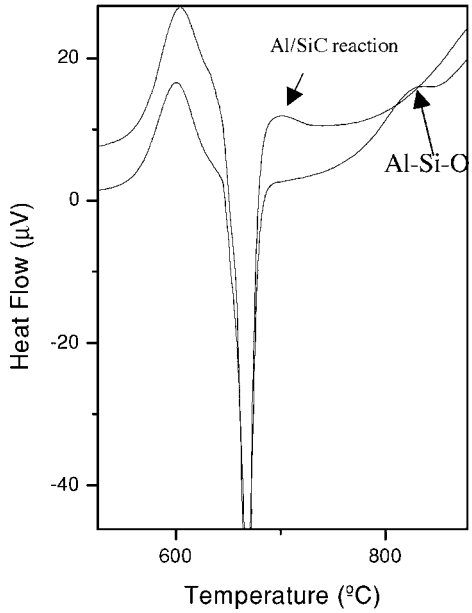

(b)

Figure 2 (a) DTA curves for Al-SiC composites with protected and unprotected particles. (b) Zoom detail of the Al/SiC and Al/SiO_2 interfacial reaction range.

3.1. Reactivity study by differential thermal analysis

Before the microstructural study of the reactive interfaces present in the particle/barrier/matrix system, DTA tests were carried out on Al-SiC_{oxd} and Al-SiC composites with the same compositions and treatments as those prepared for microscopic observation. Fig. 2 shows the superposed DTA curves of both composite materials with protected and unprotected SiC particles. Although both curves are almost coincident, and the endothermic peak of aluminium melting is clearly distinguishable, there are two main differences, which have been marked on the DTA zoom in Fig. 2b. In the DTA curve corresponding to the composite with SiC particles in as-received condition (without barrier), there is an exothermic peak corresponding to the reaction between molten Al and SiC to form Al_4C_3. The initiation temperature for this reaction is approximately 682°C. However, this peak does not appear in the DTA curve of the composite with pre-oxidized particles. In its place is another exothermic peak corresponding to another interfacial reaction, probably the formation of a glassy Al-Si-O phase by reaction between molten Al and SiO_2, which begins at temperatures close to 785°C. Table I shows the start and finish temperatures of both interfacial reactions, jointly with the changes of enthalpies measured for them.

TABLE I Temperatures and enthalpies of the interfacial reactions determined by DTA

Reaction	Start temperature (°C)	Finish temperature (°C)	Enthalpy (μV s/mg)
Al/SiC	681.6	709.7	−7.043
Al/SiO_2	795.3	849.9	−9.469

These first results show that the SiO_2 coating generated by direct oxidation of SiC particles acts as an active barrier, replacing the degradative reaction of Al_4C_3 formation with another at higher temperatures. This also implies a decrease of interfacial energy, and hence an increase in adhesion work and in wettability.

3.2. Reactivity at the Al/SiO_2 interface

After 1 h of treatment at 900°C, the TEM images of the Al/SiO_2 interfaces showed the formation of a double reaction layer approximately 800 nm thick; this had completely replaced the original SiO_2 diffusion barrier, which after oxidation treatment of the SiC particles (1200°C-2 h) was approximately 100 nm thick. Fig. 3a shows the microstructure of this double reaction layer, whose inner layer with a complex nanostructure,

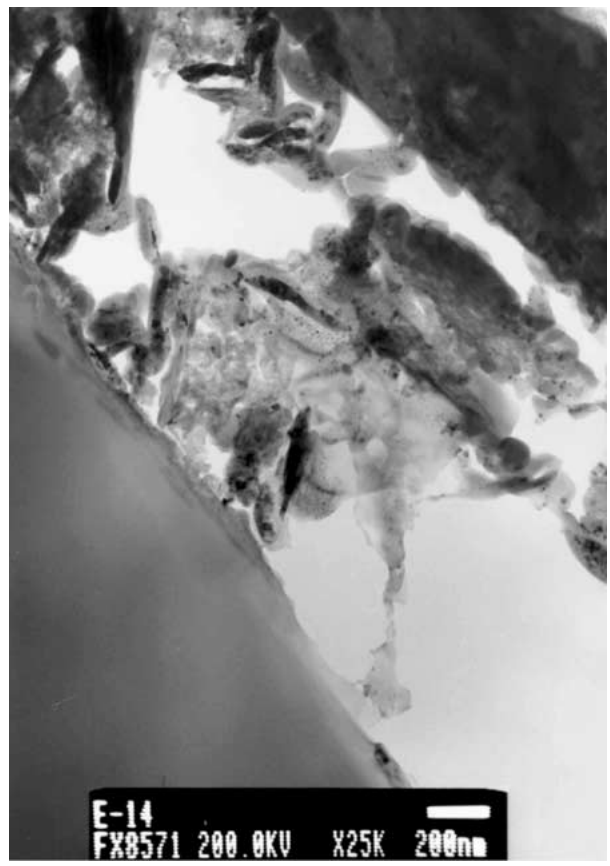

(a)

Figure 3 (a) TEM microstructure of the reaction zones between a pre-oxidized SiC particle (2 h at 1200°C) and molten aluminium (20 min at 900°C). (b) EDS of the inner Al-Si-O reaction layer. (c) EDS of the outer Al_2O_3 reaction layer. (*Continued*.)

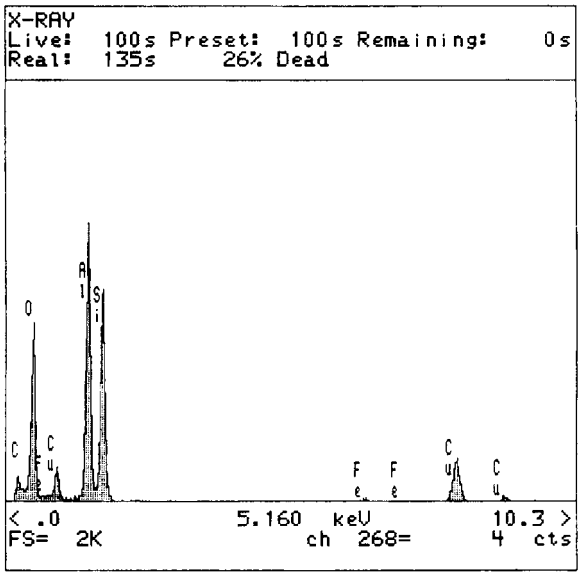

(b)

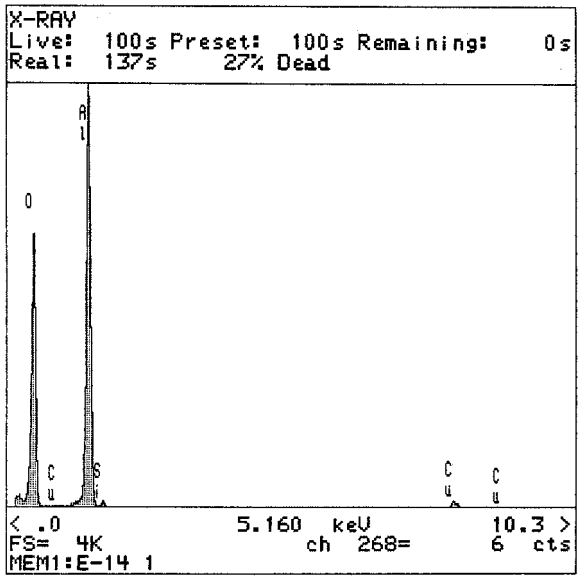

(c)

Figure 3 (*Continued*).

consists mainly of an amorphous Al-Si-O compound (Fig. 3b), while the composition of the outer layer is close to Al_2O_3 (Fig. 3c), with a nanocrystalline structure which could not be identified by electron diffraction.

For particles protected after 2 hours of oxidation treatment at 1200°C, the protection barrier was completely consumed by contact with molten aluminium for 1 h at 900°C. HREM observations (Fig. 4) showed that when this occurred, the Al-Si-O glassy phase formed by direct reaction between molten Al and SiO_2 produced preferential dissolution of the SiC. This glassy phase penetrates in a perpendicular direction to the *c* axis of the SiC, producing the special figures of dissolution which have been observed on the SiC faces in previous SEM studies [23].

By increasing the duration of the oxidation treatment (8 h at 1200°C) to obtain a thicker SiO_2 barrier, it is possible to prolong the incubation time and hence to prevent its complete consumption by interface reaction. This can be seen in Fig. 5, which shows a TEM

Figure 4 Preferential dissolution of the SiC planes by reaction with the Al-Si-O phase after consumption of the SiO_2 active barrier.

image of the interfacial microstructure formed in the contact between one of these particles and molten aluminium at 900°C during 60 min. There are two main differences with respect to the previous barrier: (1) the structure of the inner reaction layer looks more compact and presents a nanocrystalline structure, although this could not be identified by electron microdiffraction,; (2) remains of the original SiO_2 active barrier are visible between the SiC surface and the inner Al-Si-O reaction layer.

HREM images confirm both facts (Fig. 6a and b). Fig. 6a shows a detail of the SiC/Al-Si-O interface, where the $\{1\ 1\ \bar{2}\ 0\}$ crystalline planes of the SiC are distinguished by measuring their characteristic interplanar distance (14.4 Å). SiC surfaces are in contact with a narrow amorphous interphase of regular thickness (∼5 nm), which could be the remains of the SiO_2 barrier which did not react. HREM also shows the amorphous structure of the glassy Al-Si-O phase, where areas with atomic order are visible. The average distance between these atomic planes is approximately 7.66 Å, which corresponds to the b parameter of orthorhombic mullite ($3\ Al_2O_3 \cdot 2\ SiO_2$) ($a = 7,537$ Å, $b = 7,675$ Å · y $c = 2,878$ Å).

The structure of the outer reaction layer is again consistent with Al_2O_3 composition, although in this case there was also a variation in crystallinity. In the most cases, this alumina layer presented a nanocrystalline structure not resolvable by electron diffraction, but the prolongation of the reaction time up to 60 minutes favoured its crystallization to form δ-alumina (Fig. 7).

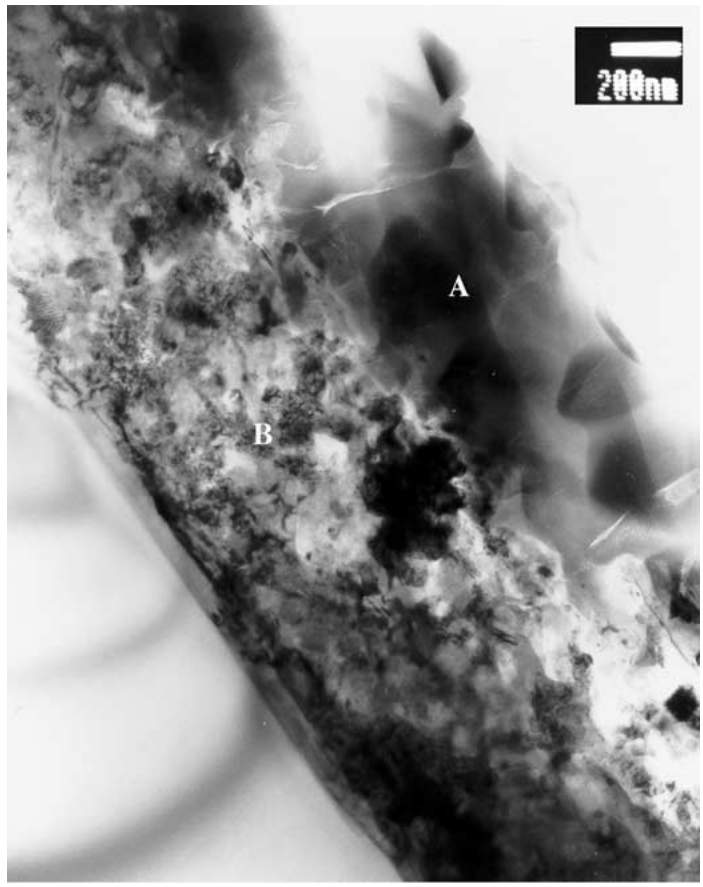

Figure 5 TEM microstructure of the reaction zones between a pre-oxidized SiC particle (at 1200°C for 8 h) and molten aluminium (900°C for 1 h).

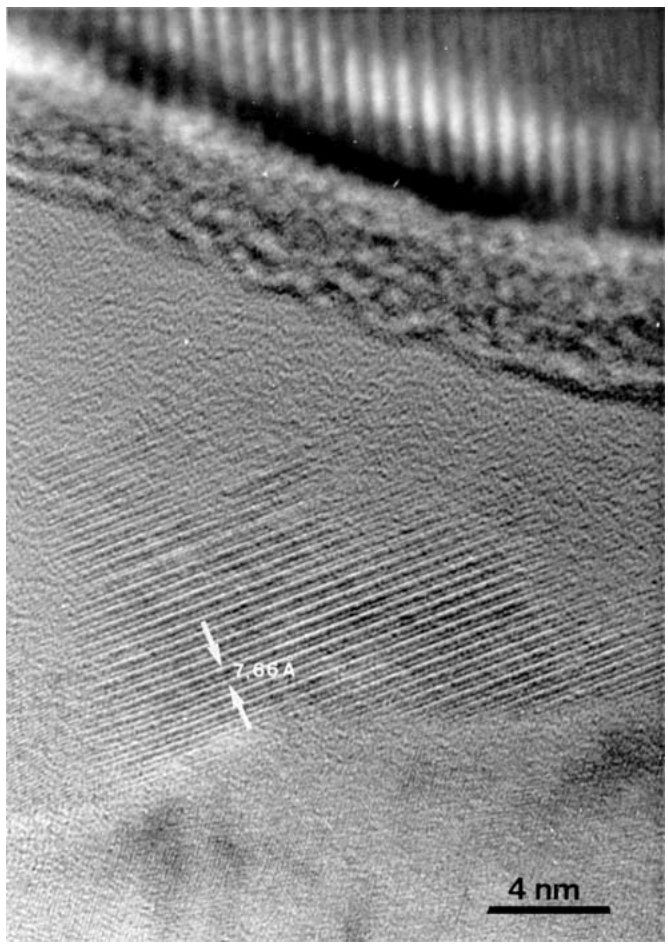

(a)

Figure 6 (a) HREM of the interface between the SiC and the Al.-Si-O glassy reaction products showing unreacted remains of the active barrier and mullite crystallization areas. (b) Crystalline aggregates formed inside the glassy Al-Si-O interphase. (*Continued*.)

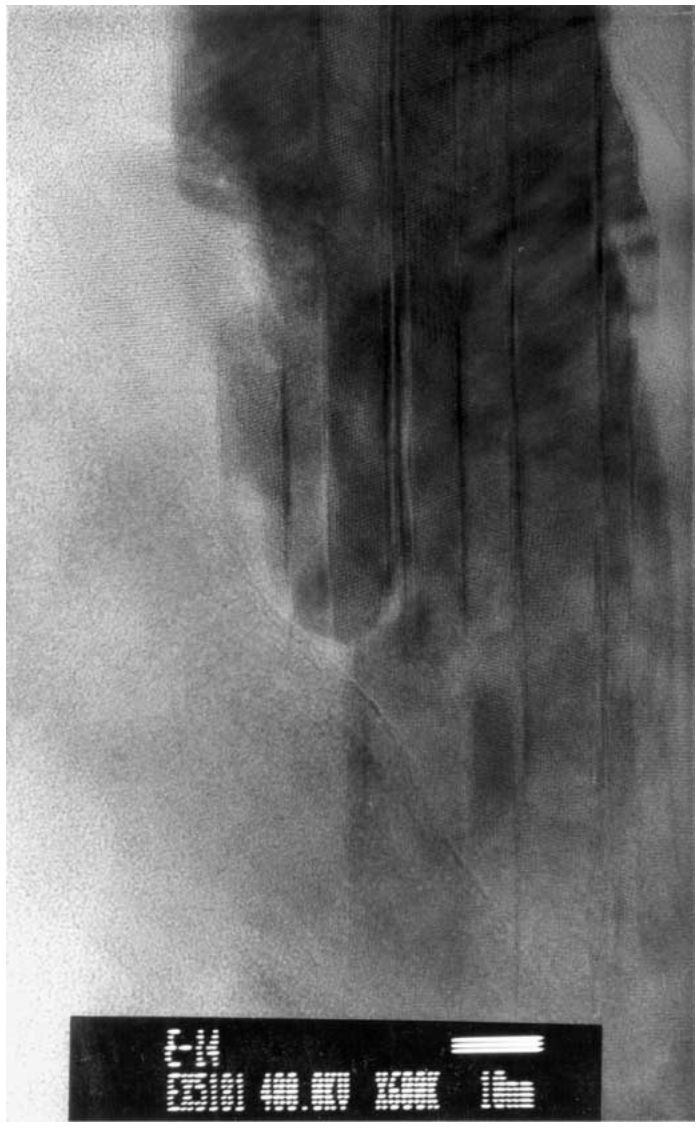

(b)

Figure 6 (*Continued*).

Another fact that was observed in specimens with non-consumed barrier was the existence of a composition gradient in the inner reaction layer. Fig. 8 shows an image of the microstructure of this zone obtained by Field Emission Microscopy (FEG-TEM) along with the EDS microanalysis of the two areas marked A and B. It follows from these that the ratio Al/Si is lower the closer one gets to the SiC surface.

3.3. Secondary reaction inside the reaction interphases

Besides the crystallization of the Al-Si-O glassy phase and the formation of δ-alumina from the amorphous phase, which can be considered as secondary transformations occurring after initial interfacial reactions between molten aluminium and SiO_2 barrier; the main secondary reactions occurred inside that glassy phase and were associated both with the dissolution effect of the glassy phase on the SiC when the barrier is consumed and with the presence of some alloy elements in the metal matrix composite.

In specimens where the protection barrier was completely consumed by reaction with the matrix constituents (SiC oxidized at 1200°C for only 2 h), TEM-EDS detected C-rich aggregates were detected inside the glassy Al-Si-O reaction interphase (Fig. 9a and b). These phases presented an amorphous structure, sizes in the range of 100–150 nm and an absence of well defined limits. Observation at higher magnifications (Fig. 9c) showed that these aggregates were constituted by a globular substructure, with particle sizes lower than 10 nm and with morphologies similar to those produced by the solidification of a eutectic liquid.

In the specimens in which the incubation time of the active barrier was passed, there was also precipitation of metallic needles of the impurities present in the aluminium matrix (mainly Cu, but also Fe) inside the inner Al-Si-O reaction layer (Fig. 3a). In most cases these aggregates appeared along with C-rich aggregates and were not detected in reaction layers in interfaces where the SiO_2 barrier had not completely reacted.

4. Discussion

The discussion of the foregoing results relates to the main objectives of the active diffusion barrier, which are:

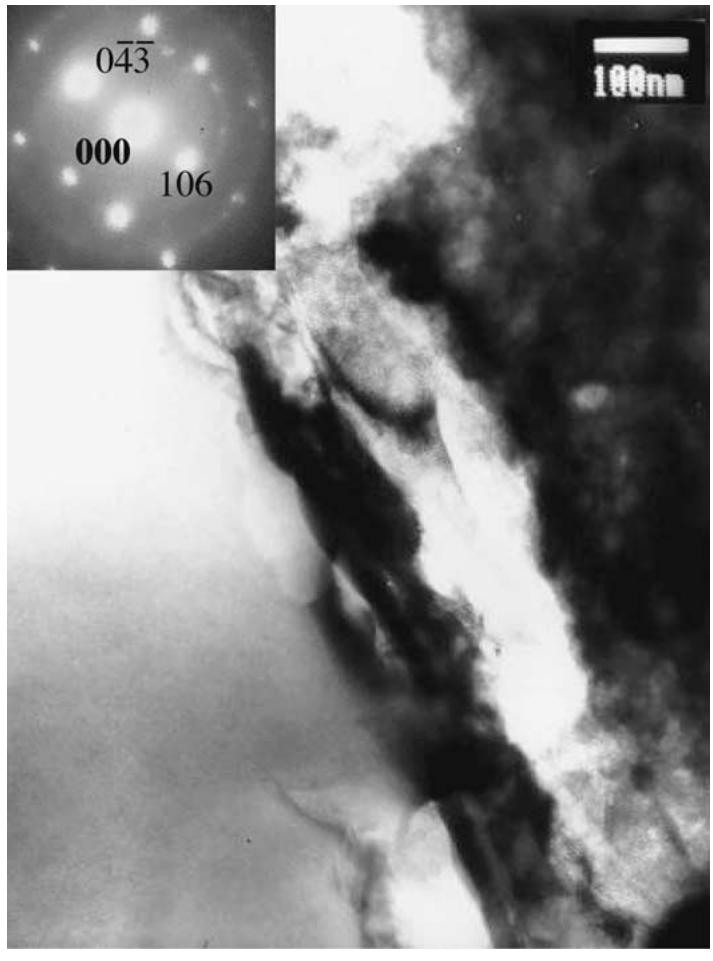

Figure 7 TEM image of an Al-SiC interface where the outer zone was identified by electron diffraction as δ-alumina.

– To prevent direct interfacial reaction between molten aluminium and silicon carbide, and hence the formation of aluminium carbide.
– To control the diffusion of Al and C through the barrier and thus prevent them reacting.
– To favour wetting of the molten aluminium on the SiC surfaces, thus increasing the liquid processability of the Al-SiCp composites.

As regards the first objective, the results show that the interposition of a SiO_2 coating between the SiC and the molten aluminium matrix replaced the direct reaction thanks to the generation of a new active interface: SiO_2-Al. It was in this interface that new reactions were generated, the main interfacial product being a glassy Al-Si-O compound which was probably generated in the liquid phase and solidified after. The microstructure of the interface reaction compounds and its evolution were mainly conditioned by the time of contact between the molten aluminium and the active barrier. When this was longer than the incubation time, which depended on thickness (oxidation time), the SiO_2 coating was consumed and the interface reaction affected the SiC. However, even in these cases the formation of Al_4C_3 was avoided.

From these results, a model was constructed to explain the mechanisms of interface reaction, also considering two alternative possibilities: consumption or otherwise of the active diffusion barrier. Fig 10a and b summarize both situations, considering the participation of further stages in the proposed models:

4.1. Interface reactions without complete consumption of the barrier

4.1.1. Stage I: reaction of alumino-silicate formation

The first reaction that occurred between the barrier and the molten aluminium was the formation of glassy alumino-silicates in the SiO_2/Al interface. This can be established by the following general reaction as:

$$y\,SiO_2 + x\,Al \rightarrow Al_x\,Si_yO_z \quad (z = 2y) \qquad (1)$$

It can be deduced from the DTA tests that this reaction completely replaced the Al_4C_3 forming reaction and occurred at almost 200°C more than the temperature of direct reaction between molten Al and SiC. In the test conditions, the temperature at the onset of $Al_xSi_yO_z$ formation was 785°C as compared to 682°C for the Al_4C_3 reaction. Both reactions are exothermic, which favours a decrease of interfacial energy and hence wetting behaviour.

4.1.2. Stage II: reaction of alumina formation

The alumina formation at the outer reaction layer could be associated with the following reaction:

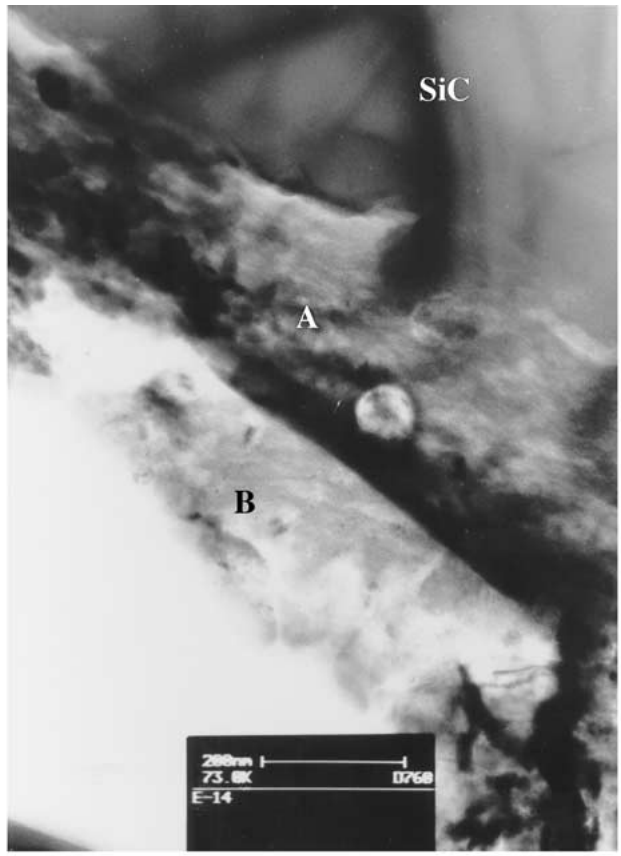

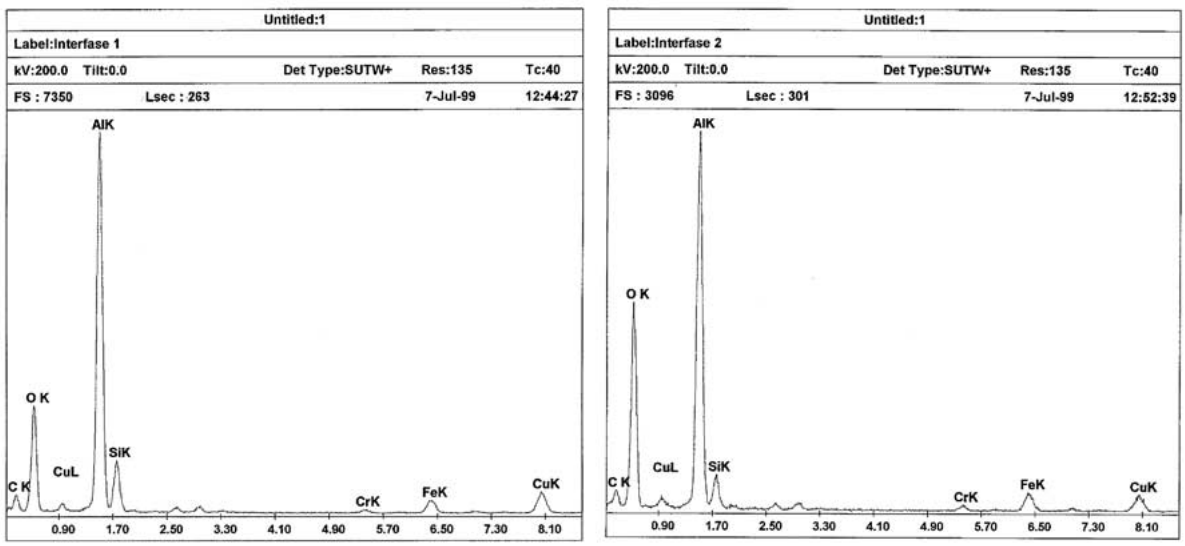

Figure 8 Field emission electron micrograph showing a detail of the inner Al-Si-O reaction interphase. (a) EDS microanalysis of the zone marked A. (b) EDS microanalysis of the zone marked B.

$$SiO_2 + 4/3Al \rightarrow 2/3Al_2O_3 + Si$$
$$\Delta G^{o}_{900^{\circ}C} = -168,513\,kJ \qquad (2)$$

In previous studies carried out by Hughes *et al.* [24] on reactivity in $Al/SiO_2/SiC$ interfaces, it was shown that the formation of alumina by the previous reaction only occurred when a very thin coating of SiO_2 was used, and only once all the silica was consumed. However, the present studies show that it formed even in those interfaces where SiO_2 was not completely consumed. But it is important to note that the trial conditions tested by Hughes *et al.* were quite different; they used single crystals of SiC-6H which had previously been oxidized at 600°C (unlike in the present studies where the polycrystalline SiC particles were oxidized at 1200°C). Also, the reaction with molten aluminium was achieved by coating the treated SiC surface with a thin film (∼1 nm) of pure aluminium and heating at 800°C.

The detection of the alumina reaction layer even in those interfaces where the SiO_2 barrier was not consumed could also be associated with the presence of occluded O_2 inside the remaining pores of the powder compacted specimens. This oxygen would favour the following reaction between the glassy phase and the molten aluminium:

$$Al_xSi_yO_z + xAl + mO_2 \rightarrow xAl_2O_3 + ySi$$
$$(\text{for } z + 2m = 3x) \quad (3)$$

The presence of excess oxygen (i.e., if the melting tests were not carried out under high vacuum) would produce a direct reaction between aluminium and oxygen, forming a continuous layer of alumina which would prevent subsequent wetting and the progression of the interfacial reactions.

(a)

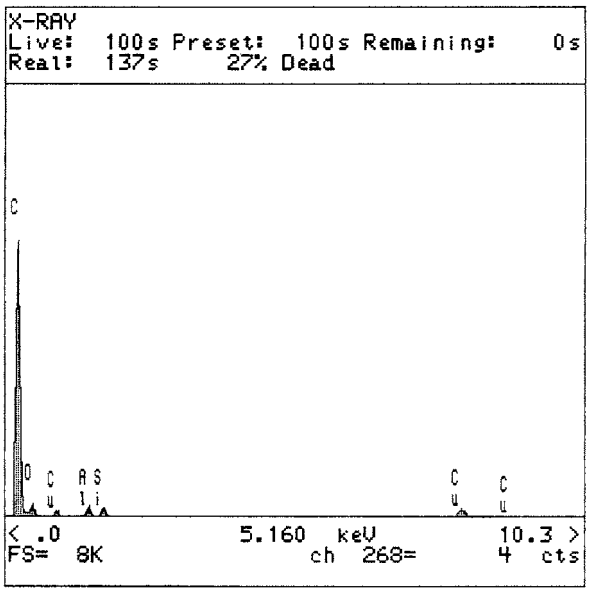

(b)

Figure 9 (a) TEM image of a C-rich aggregate inside the Al-Si-O glassy phase. (b) EDS of this aggregate. (c) Detail of the nanoglobular structure of these aggregates at higher magnification. (*Continued*.)

(c)

Figure 9 (*Continued*).

TEM observation showed that the alumina layer formed by the previous reactions had a nanocrystalline structure with a grain size too small to be resolved by electron microdiffraction. However, in specimens where the contact between molten aluminium and protected SiC particles was more prolonged (60 min), there was an increase in grain size and this outer layer was identified as δ-alumina.

4.1.3. Stage III: crystallization of inner glassy phase

In those interfaces where the SiO_2 active diffusion barrier was not completely consumed, it was observed that $Al_xSi_yO_z$ glassy phase tended to crystallize and form mullite, which generates more compact interfaces. Previous studies carried out by Low *et al*. [26] consider that crystallisation of mullita from an alumino-silicate glassy phase occur in several stages, generating first a spinel-like ordered structure (pre-mullite), prior the subsequent nucleation of the orthorhombic structure of the mullite.

Although TEM observations in present study have not detected the formation of this spinel-like structure from the glassy phase; however, the HREM images did detect the formation of ordered zones with the characteristic parameters of mullite, being its formation favoured prolonging the reaction time. The differences in composition (Al/Si rate) detected by EDS microanalysis in this reaction layer were also within the range of composition of this phase, being richer in SiO_2 close to the barrier and richer in Al_2O_3 closer to the matrix.

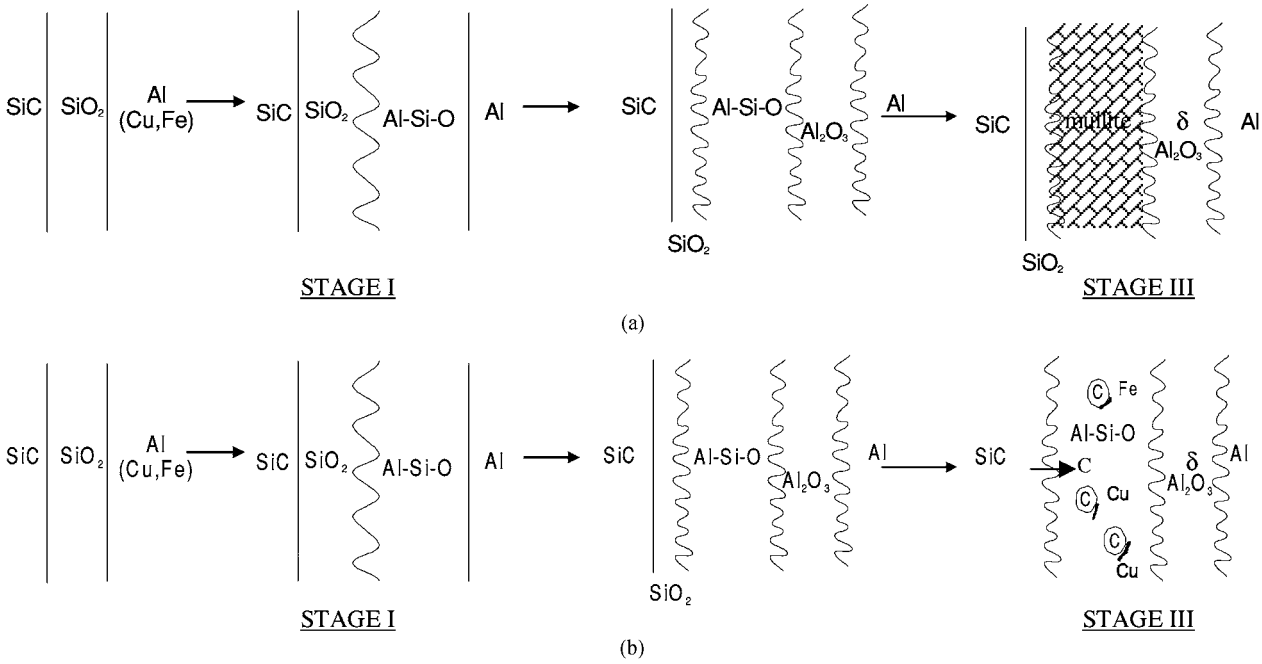

Figure 10 Schemes of the proposed reaction models for the SiO_2 active diffusion barrier in the Al-SiC system. (a) Stages in systems where barrier is not completely consumed. (b) Stages in systems where barrier is completely consumed.

Hence, the complete reaction of mullite formation could be expressed as:

$$SiO_2 + 12/13Al \rightarrow 2/13\,(3Al_2O_3 \cdot 2SiO_2) + 9/13\,Si$$
$$\Delta G^{o}_{900^{\circ}C} = -118,908\,kJ \quad (4)$$

4.2. Interface reactions with complete consumption of the active barrier

However, in those cases where the active barrier was not thick enough and was completely consumed by reaction (1), it was observed that the glassy Al-Si-O phase dissolved in preferential directions to the SiC, thus changing the structure and composition of the inner interfacial layer. Stages I and II, then, would have occurred in the same way as in the previous model, but where the reaction time is longer than the barrier incubation time, stage III is as follows:

4.2.1. Stage III: dissolution of SiC particles

Although the models proposed by other authors [24] consider that Al_4C_3 formation takes place once the SiO_2 has been consumed, the results of the present research show that the consumption of the active diffusion barrier is followed by etching of the SiC by the glassy Al-Si-O reaction phase, without subsequent formation of Al_4C_3.

This chemical etching produces a dissolution effect which is favoured in certain crystalline planes of the SiC. The result is C-enrichment of the glassy Al-Si-O phase, which favours the formation of amorphous carbon aggregates with a nanoglobular structure. The presence of free amorphous carbon inside the Al-Si-O reaction layer supports the hypothesis that it is formed during the interfacial reaction, once the active SiO_2 barrier is consumed, by the reaction:

$$SiC + Al_xSi_yO_z + O_2 \rightarrow mAl_2O_3 + nSiO_2 + C \quad (5)$$

although the amorphous carbon aggregates could be formed as reaction products associated with mullite formation, by means of the reaction:

$$2SiC + 3Al_2O_3 + 2O_2 \rightarrow 3Al_2O_3 \cdot 2SiO_2 + 2C \quad (6)$$

However, the C-rich aggregates were mainly associated with the glassy Al-Si-O and only exhibited a minority presence in those interfaces where crystallization to mullite was more favoured. Nevertheless, both reactions require the presence of oxygen, which is not entirely infeasible given the high residual porosity of the compacted Al-SiC powder specimens. C formation would be favoured by the low O_2 partial pressure of the reaction zone.

The particular nanostructure of these carbon aggregates is similar to some pseudoeutectic microstructures. This could explain the possible formation of the C aggregates from a eutectic liquid in an Al-Si-O-C solution, proposed by Mortesen and Jin to explain the transformations during the joining of SiC with Al solders [27].

Another secondary transformation that was detected is the precipitation of metallic needles of Cu and Fe inside the inner Al-Si-O, which is associated with the formation of amorphous C aggregates. These metallic elements diffuse from the metallic matrix where they are present as impurities, and they are stopped by the active barrier where they precipitate. The reduction effect of the free carbon present in this reaction layer would favour its precipitation as reduced phases.

5. Conclusions

1. The SiO_2 coating generated by oxidation of the SiC particles for 8 h at 1200°C acts as an active diffusion barrier in contact with molten aluminium, due to the interfacial reaction between them, which generates mainly alumino-silicate phases and alumina.

2. The reaction between the barrier and the molten aluminium is an exothermic one and occurs at approximately 785°C, which is roughly 100°C more than the temperature of Al_4C_3 formation when unprotected SiC particles react with molten aluminium.

3. In the experimental conditions, the primary reaction between the active barrier and the molten aluminium generates a glassy phase ($Al_xSi_yO_z$) which is liquid at the tested reaction temperature (900°C). This phase tends to crystallize, forming nanocrystalline mullite which increases the interfacial stability.

4. The consumption of the SiO_2 protective barrier for the studied reaction conditions (900°C, 20 and 60 min), which occurs in barriers obtained by only 2 h of oxidation treatment, does not cause the formation of Al_4C_3 but preferential dissolution of the SiC and subsequent formation of amorphous C-rich aggregates with a nanoglobular structure inside the glassy Al-Si-C phase.

5. The carbon enrichment of the alumino-silicate interphase inhibits its crystallization to mullite and activates precipitation of the metallic elements present as impurities in the aluminium matrix.

Acknowledgements

The authors wish to thank to the *Comision Interministerial de Ciencia y Tecnología* (CICYT) for the financial support given to this research (project MAT2000-1646-C02-01). We also wish to thank Navarro S.A. for supplying the SiC particles.

References

1. P. MOGILEVSKY, A. WERNER and H. J. DUDEK, *Mater. Sci. Eng.* A **242** (1998) 235.
2. V. LAURENT, D. CHATAIN and N. EUSTATHOPOLOUS, *ibid.*, *135* (1991) 89.
3. Z. FAN, Z. X. GUO and B. CANTOR, *Composites Part A: Applied Science and Manufacturing* **28** (1997) 131.
4. L. C. KWANG and B. DERBY, in Proceedings of Topical Symposium III Advanced Fiber Composites of the 8th CIMTEC-World Ceramics Congress and Forum on New Materials. 28 June–4 July 1994; Florence, Italy, p. 179.
5. S. Q. GUO, Y. KAGAWA, Y. TANAKA and C. MASUDA, *Acta Materialia*, **46** (1998) 4941.
6. S. M. JENG, J. M. YANG and J. A. GRAVES, *J. Mater. Res.* **8** (1993) 905.
7. T. D. MCGARRY, M. J. PINDERA and F. E. WAWNER, *Composites Engineering* **5** (1995) 951.
8. B. S. MAJUMDAR, *Materials Science and Engineering* **259** (1999) 171.
9. A. UREÑA, J. M. GÓMEZ DE SALAZAR, L. GIL, M. D. ESCALERA and J. L. BALDOMERO, *Journal of Microscopy* **196** (1999) 124.
10. A. UREÑA, P. RODRIGO, L. GIL, M. D. ESCALERA and J. L. BALDONEDO, *J. Mater. Sci.* **36** (2001) 419.
11. *Idem.*, *ibid.* **36** (2001) 429.
12. J. P. ROCHER, J. M. QUENISSET and R. NASLAIN, *ibid.* **24** (1989) 2697.
13. Y. L. LIU and B. KINDL, *Scripta Metallurgica et Materialia*, **27** (1992) 1367.
14. B. KINDL, Y. H. TENG and Y. L. LIU, *Composites* **25** (1994) 671.
15. M. SUERY, G. L'ESPERANCE, B. D. HONG, L. NGUYEN-THANH and F. BORDEAUX, *J. Mater. Eng. and Perform.* **2** (1993).
16. P. TRESPAILLE-BARRAU and M. SUERY, *Materials Science and Technology* **10** (1994) 497.
17. J. C. LEE, J. I. LEE and H. I. LEE, *J. Mater. Sci. Lett.* **15** (1996) 1539.
18. K. T. KIM, M. W. KO and C. H. LEE, *Journal of the Korean Institute of Metals and Materials* **31** (1993) 1487.
19. R. ASTHANA and P. K. ROHATGI, *J. Mater. Sci. Lett.* **12** (1993) 442.
20. W. S. CHUNG, S. Y. CHANG and S. J. LIN, *Plating & Surface Finishing* **83** (1996) 68.
21. A. MANZANO, E. NAVA and C. VAZQUEZ, *Scripta Metallurgica et Materialia* **29** (1993) 1241.
22. R. ASTHANA and P. K. ROHATGI, *Key Engineering Materials* **79/80** (1993) 47.
23. A. UREÑA, E. E. MARTÍNEZ, E. CRIADO and L. GIL, *Mater. Sci. Tech.*, in press.
24. A. E. HUGHES, M. M. HEDGES and B. A. SEXTON, *J. Mater. Sci.* **25** (1990) 4856.
25. J. WEISS, H. L. LUKAS, J. LORENZ, G. PETZOW and H. KRIEG, *CALPHAD: Comput. Coupling Phase Diagrams Thermochem.* **5** (1981) 125.
26. I. M. LOW and R. MCPHERSON, *J. Mater. Sci.* **24** (1989).
27. A. MORTESEN and Y. JIN, *Int. Mat. Reviews*. **37** (1992) 101.

Received 17 October 2001
and accepted 3 June 2002